J. Vet. Sci. (2009), **10**(4), 299–304
DOI: 10.4142/jvs.2009.10.4.299

JOURNAL OF
Veterinary
Science

Infrared spectroscopy characterization of normal and lung cancer cells originated from epithelium

So Yeong Lee[1], Kyong-Ah Yoon[2], Soo Hwa Jang[1], Erdene Ochir Ganbold[3], Dembereldorj Uuriintuya[3], Sang-Mo Shin[4], Pan Dong Ryu[1], Sang-Woo Joo[3,*]

[1]*Laboratory of Pharmacology, College of Veterinary Medicine, Seoul National University, Seoul 151-742, Korea*
[2]*Research Institute and Hospital, National Cancer Center, Goyang 410-769, Korea*
[3]*Department of Chemistry, Soongsil University, Seoul 156-743, Korea*
[4]*Department of Mechatronics, Gwangju Institute of Science and Technology, Gwangju 500-712, Korea*

The vibrational spectral differences of normal and lung cancer cells were studied for the development of effective cancer cell screening by means of attenuated total reflection infrared spectroscopy. The phosphate monoester symmetric stretching $\nu_s(PO_3^{2-})$ band intensity at ~970 cm^{-1} and the phosphodiester symmetric stretching $\nu_s(PO_2^-)$ band intensity at ~1,085 cm^{-1} in nucleic acids and phospholipids appeared to be significantly strengthened in lung cancer cells with respect to the other vibrational bands compared to normal cells. This finding suggests that more extensive phosphorylation occur in cancer cells. These results demonstrate that lung cancer cells may be prescreened using infrared spectroscopy tools.

Keywords: cancer cell screening, cell monitoring, infrared spectroscopy, lung cancers, phosphorylation

Introduction

Cancer is the principal causes of death worldwide according to the World Health Organization, with lung cancer being one of the most commonly diagnosed types of cancer in men and the fourth most common cause of cancer-related death in men [18]. The early detection of invasive lung cancer is essential in reducing its mortality rate. It has been problematic, however, to determine the quantitative differences in spectral signatures between normal, precancerous, and cancer cells without causing structural and biochemical changes.

One of the most popular diagnostic methods in the clinical assessments of various cancers may be the microscopic evaluation of a stained biopsy for a specific organ by pathologists [4]. However, efforts have been made to improve the early detection rate using spectroscopic methods [7]. Optical spectroscopy such as Raman [2], infrared [4], and fluorescence [21] has been shown to be able to discriminate between normal and malignant tissues for many cancers. However many physical methods of cancer analysis are yet either inaccurate or costly.

Infrared vibrational spectroscopy can provide valuable information about the structure and composition of various biological materials [4] and has been recently applied to not only food sciences, but also the veterinary field [10]. Fourier-transform infrared spectroscopy (FT-IR) has been applied to a variety of phenomena in the biomedical sciences with fast, automated-data acquisition time and is inexpensive. The advances in FT-IR technology make it possible to detect inflammatory and precancerous cell states with the advantages of a rapid measuring process and high spatial resolution. This technique enables the study of the state of chemical bonds and the relative concentrations of lipids, proteins, carbohydrates, and phosphorylated compounds [5].

There have been relatively few reports [3,5,6,11,13-17, 19,22,24] monitoring the morphology of cancer cells using vibrational spectroscopic tools. Although there have been several infrared spectroscopy studies [20,23] on lung cancer cell lines, a detailed analysis on the congested spectral features has not yet been performed. In this study, we examined the phosphate stretching region using a peak fitting program revealing various spectral peaks of lung cancer cell lines to better discriminate between the normal and lung cancer cells. The vibrational spectra of lung cancer cells were analyzed by attenuated total reflection infrared spectroscopy in order to screen for structural and intracellular alterations in lung cancer cells compared to normal human bronchial epithelial cells.

*Corresponding author
Tel: +82-2-820-0434; Fax: +82-2-820-0434
E-mail: sjoo@ssu.ac.kr

Materials and Methods

Cell culture and sample preparation for infrared spectroscopy

NCI-H358 and NCI-H460 lung cancer cells were grown on RPMI 1640 (Gibco, USA). The normal human bronchial epithelial (NHBE) cells were obtained from Cambrex (USA) and maintained in bronchial epithelial growth medium. All cells were supplemented with 10% fetal bovine serum and ×1 penicillin-streptomycin antibiotics (Gibco, USA) and maintained in 5% CO_2/95% humidified air at 37°C.

Approximately 5×10^3 cells were washed with phosphate buffer saline and 0.25% trypsin-EDTA was added for 10 min to detach the cells. After centrifugation at 1,200 rpm for 10 min, the supernatant was discarded and washed using phosphate buffered saline. The saline specimens were centrifuged at 3,000 rpm for several minutes and cell pellets were transferred to a microcentrifuge and centrifuged at 5,000 rpm for 10 min to provide a small pellet of cells for FT-IR analysis [19].

Characterization of normal and lung cancer cells

The NCI-H460 lung cancer cells originated from a patient with large cell cancer of the lung (ATCC catalog number: HTB-177), which makes up approximately 10-20% of lung cancers. The NCI-H358 lung cancer cells were derived from a primary bronchioalveolar carcinoma of the lung from a Caucasian patient (ATCC catalog number: CRL-5807). Primary NHBE cells were used as normal lung cells.

Infrared measurements

The infrared spectra were obtained using a FT-IR spectrometer with a maximum resolution of 0.09 cm^{-1} (Thermo Nicolet 6700) equipped with a liquid N_2 cooled HgCdTe detector [12]. A total of 128 scans were measured in the range of 1,000-3,500 cm^{-1} with a resolution of 4 cm^{-1}. The prepared lung cancer cell pellet was transferred onto a ZnSe crystal of Pike Technology Miracle external reflection accessory. Data processing was carried out using the OMNIC v5.1a software (Thermo Scientific, USA). Spectral parameters and fitting of each spectrum was obtained using a PeakFit version 4.12 (Systat, USA).

Results

Infrared spectra of normal lung cells

Fig. 1a shows the mid-infrared spectra of normal lung cells. Among several vibrational features, the amide I band at ~1,650 cm^{-1} was due primarily to the C = O stretching vibrational bands of the peptide backbone. The amide II band at ~1,550 cm^{-1}, due largely to a coupling of CN stretching and in-plane bending of the N-H group, was also found to be fairly strong in the infrared spectrum. The two vibrational bands at ~1,460 and ~1,400 cm^{-1} could be ascribed to the in-plane bending vibrations of CH_3. On the

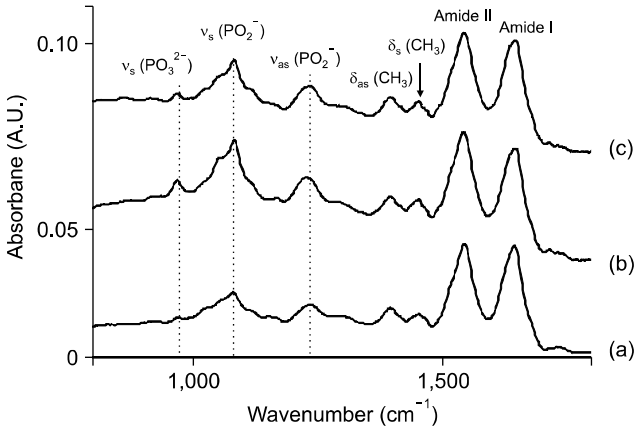

Fig. 1. Infrared spectra of (a) normal human bronchial epithelial (NHBE) and (b) NCI-H358 and (c) NCI-H460 lung cancer cells. The spectra for each sample were read twice to check reproducibility. The intensities were normalized with respect to that of the amide I band at ~1,650 cm^{-1}.

Table 1. Spectral data and vibrational assignments of normal and lung cancer cells*

Normal cells (NHBE†)	Cancer cells (NCI-H358)	Cancer cells (NCI-H460)	Assignment‡
1,649	1,648	1,645	Amide I
1,548	1,549	1,548	Amide II
1,456	1,456	1,456	Methyl groups $\delta_s(CH_3)$
1,400	1,399	1,400	Methyl groups $\delta_{as}(CH_3)$
1,235	1,236	1,239	$\nu_{as}(PO_2^-)$
1,084	1,086	1,085	$\nu_s(PO_2^-)$
972	970	971	$\nu_s(PO_3^{2-})$

*Unit (cm^{-1}). The frequency positions were located at the center of the mixed two bands in Fig. 3. †NHBE: normal human bronchial epithelial. ‡Based on Meurens *et al*. [15] and Zenobi *et al*. [26].

Table 2. Intensity ratios with respect to the amide I band

Normal cells (NHBE)	Cancer cells (NCI-H358)	Cancer cells (NCI-H460)	Assignment*
1.00	1.00	1.00	Amide I
0.814	0.815	0.881	Amide II
0.124	0.168	0.152	Methyl groups $\delta_s(CH_3)$
0.168	0.171	0.191	Methyl groups $\delta_{as}(CH_3)$
0.168	0.234	0.231	$\nu_{as}(PO_2^-)$
0.274	0.556	0.426	$\nu_s(PO_2^-)$
0.0318	0.140	0.0686	$\nu_s(PO_3^{2-})$

*Based on Meurens *et al*. [15] and Zenobi *et al*. [26].

other hand, the vibrational bands at ~1,235 and ~1,085 cm^{-1} were assumed to belong to the stretching modes of the PO_2^- group. The weak vibrational band at ~970 m^{-1} could be ascribed to the PO_3^{2-} group. Our assignment was listed in Table 1.

Infrared spectra of lung cancer cells

The infrared spectra of lung cancer cells were recorded as shown in Figs. 1b and c. It is noteworthy that the $\nu_s(PO_3^{2-})$ and $\nu_s(PO_2^-)$, bands at ~970 and ~1,085 cm^{-1}, respectively, appeared to be greatly intensified for the two cancer cells in comparison with normal lung cells. These bands were found to be the most enhanced for the NCI-H358 cells derived from a primary bronchioalveolar carcinoma of the lung. It is remarkable that the spectral difference could be clearly observed by direct observation of several vibrational bands in the present study. The relative intensities with respect to the amide I band are summarized in Table 2. Fig. 2 shows histograms for the three lung cells of several vibrational band intensities. An expanded view of infrared spectra in the wave number range of 900 ~ 1,290 cm^{-1} for normal and lung cancer cells are shown in Fig. 3. There were quite a few spectral features curve fitting under 900 ~ 1,290 cm^{-1} for normal and lung cancer cells (Fig. 3). In addition to the $\nu_s(PO_3^{2-})$ and $\nu_s(PO_2^-)$, bands at ~970 and ~1,085 cm^{-1}, respectively, there were also bands observed at 916, 1,029, 1,056, 1,118, and 1,155 cm^{-1}. These bands could be correlated as carbohydrates or glycoconjugates. In addition, the $\nu_{as}(PO_2^-)$ band at ~1,235 cm^{-1} can be decomposed to the two bands at 1,221 and 1,244 cm^{-1}. One of these two bands may be ascribed to the torsional mode of CH_2. These bands were also found to be slightly different from the normal or lung cancer cells as shown in Fig. 3. It is noteworthy that the bands at ~1,030 and ~1,155 cm^{-1} were relatively more enhanced for the normal cell.

Discussion

In the present study, the symmetric $\nu_s(PO_2^-)$ band at ~1,085 cm^{-1} and the phosphate monoester symmetric stretching $\nu_s(PO_3^{2-})$ band intensity at ~970 cm^{-1} were intensified in lung cancer cells compared to normal lung cells. This may be attributed to structural changes in DNA or volume density. A similar phenomenon was reported by Gazi *et al*. [5] and Maziak *et al* [14]. According to Gazi *et al*. [5] the $\nu_s(PO_2^-)$ bands at ~1,085 cm^{-1} were intensified in prostate cancer tissues compared to normal prostate epithelial cells. The frequency positions of the $\nu_s(PO_2^-)$ and $\nu_{as}(PO_2^-)$ bands were also shifted in malignant esophagus tissue [14].

In addition, the relative intensity factors of *Absorbance* $\nu_s(PO_3^{2-})$/*Absorbance* (amide I) or *Absorbance* $\nu_s(PO_2^-)$/*Absorbance* (amide I) could be used to discriminate lung cancer cells from normal cells. It is worthwhile to note that the intensities of the amide I bands appeared to be always stronger than those of the amide II band without indicating serious artifact or spectral contamination due to the dispersion effect in the reflection method as previously published in our spectral features, [17]. The glycogen level is assumed to decrease during carcinogenesis, resulting in a decrease in their intensities as previous reported [24]. It seems clear that the $\nu_s(PO_3^{2-})$ and $\nu_s(PO_2^-)$ bands at ~970 and ~1,085 cm^{-1}, respectively, may provide significant differences between normal and lung cancer cells. Based on the spectral data, our conclusions appeared to be consistent with several previous reports [20,23]. In this work we mainly focus on the analyses of multiple spectral features in the infrared spectra of lung cancer cells. Protein phosphorylation is involved in many cellular regulatory processes [8]. For example, the phosphorylation of p53, which is a tumor suppressor, is important in the regulation of p53 activities [9]. In tumor cells, deregulation, including the phosphorylation modification of p53, is frequently observed in tumor cells and known to be associated with tumorigenesis [1,25].

There are several tools to identify cancer cells and cancer diagnosis. Compared to the established techniques, the IR method is relatively inexpensive, fast and can be automated.

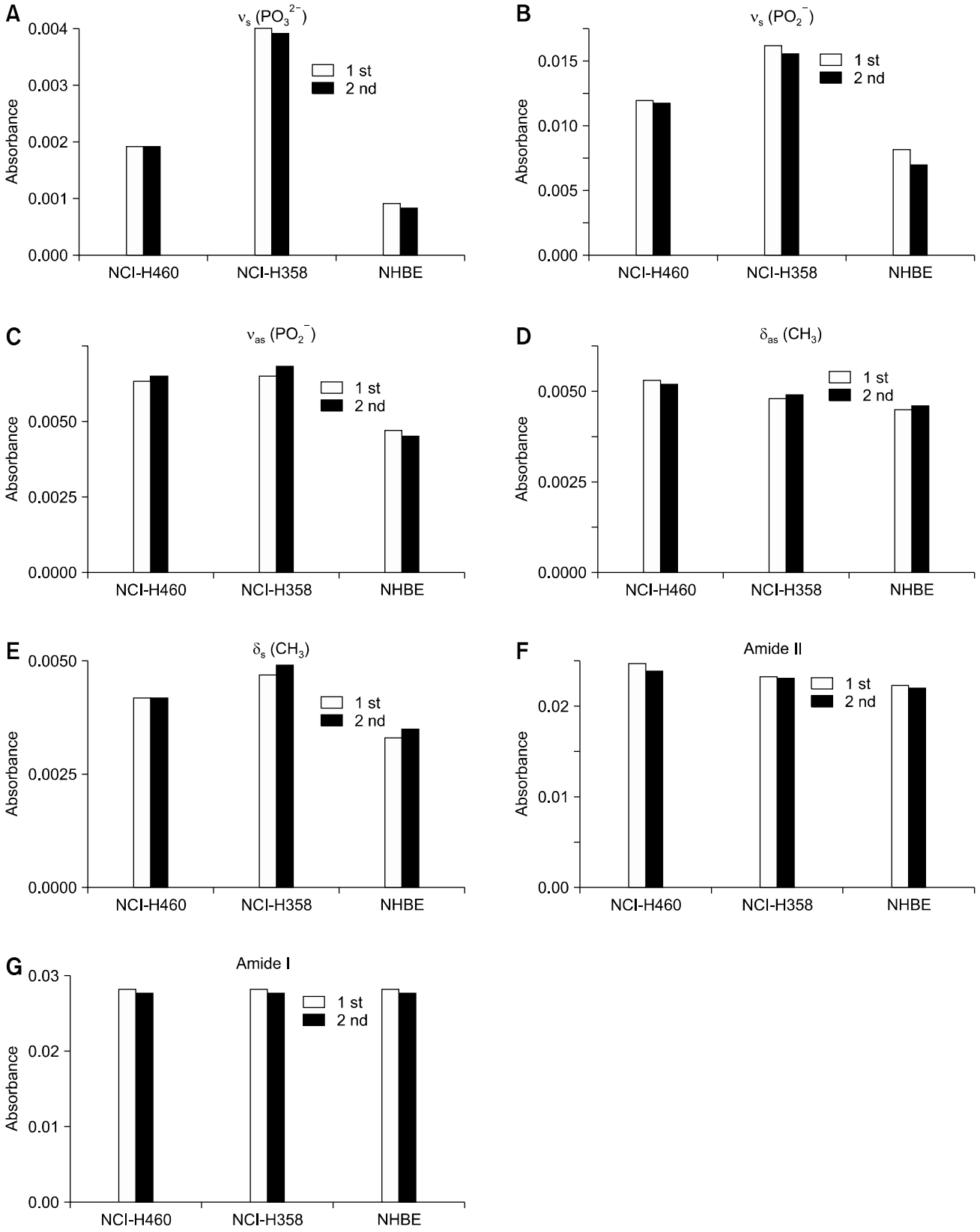

Fig. 2. Relative band intensities for NCI-H358 and NCI-H460 lung cancer cells and normal NHBE-P5 cells for (a) $\nu_s(PO_3^{2-})$, (b) $\nu_s(PO_2^-)$, (c) $\nu_{as}(PO_2^-)$, (d) $\delta_{as}(CH_3)$, (e) $\delta_s(CH_3)$, (f) amide II, and (g) amide I bands. The intensities were normalized for the amide I bands at ~1,650 cm^{-1}.

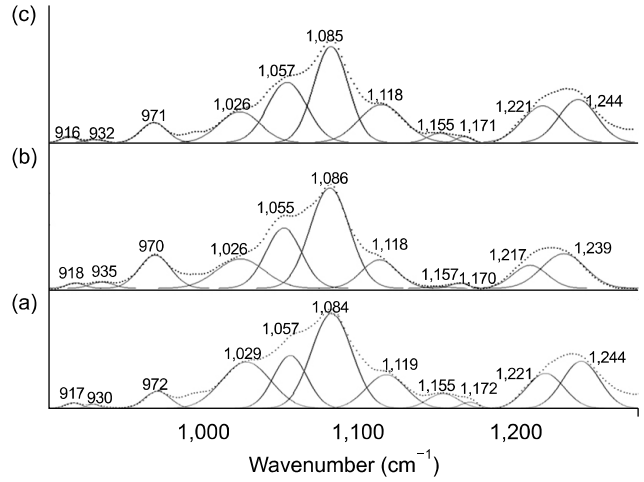

Fig. 3. Spectral curve fitting of (a) NHBE and (b) NCI-H358 and (c) NCI-H460 lung cancer cells in the wavenumber region of 900 ~ 1,290 cm^{-1}. Each sample was tested twice to check the spectral reproducibility. The y-axis scale is the *absorbance* in arbitrary units.

Moreover, it checks cells in their natural state without the need for fixation and/or staining [4,19].

In the present study, it was found that the phosphate and phosphodiester stretching bands clearly discriminated between normal and primary bronchioalveolar carcinoma cells. These results suggest that greater phosphorylation occurs in lung cancer cells compared to normal bronchial epithelial cells. Taken together, these results demonstrate that lung cancer cells may be prescreened by means of infrared spectroscopy based tools.

Acknowledgments

This research was supported by National Research Foundation Grant (2009-0066580).

References

1. **Bode AM, Dong Z.** Post-translational modification of p53 in tumorigenesis. Nat Rev Cancer 2004, **4**, 793-805.
2. **Choi J, Choo J, Chung H, Gweon DG, Park J, Kim HJ, Park S, Oh CH.** Direct observation of spectral differences between normal and basal cell carcinoma (BCC) tissues using confocal Raman microscopy. Biopolymers 2005, **77**, 264-272.
3. **Cohenford MA, Rigas B.** Cytologically normal cells from neoplastic cervical samples display extensive structural abnormalities on IR spectroscopy: Implications for tumor biology. Proc Natl Acad Sci USA 1998, **95**, 15327-15332.
4. **Dukor RK.** Vibrational spectroscopy in the detection of cancer. In: Chalmers JM, Griffiths PR (eds.). Handbook of Vibrational Spectroscopy. Vol. 5. pp. 3335-3361, Wiley, New York, 2002.
5. **Gazi E, Dwyer J, Lockyer NP, Gardner P, Shanks JH, Roulson J, Hart CA, Clarke NW, Brown MD.** Biomolecular profiling of metastatic prostate cancer cells in bone marrow tissue using FTIR microspectroscopy: a pilot study. Anal Bioanal Chem 2007, **387**, 1621-1631.
6. **Hammiche A, German MJ, Hewitt R, Pollock HM, Martin FL.** Monitoring cell cycle distributions in MCF-7 cells using near-field photothermal microspectroscopy. Biophys J 2005, **88**, 3699-3706.
7. **Hirsch FR, Franklin WA, Gazdar AF, Bunn PA Jr.** Early detection of lung cancer: clinical perspectives of recent advances in biology and radiology. Clin Cancer Res 2001, **7**, 5-22.
8. **Hunter T, Karin M.** The regulation of transcription by phosphorylation. Cell 1992, **70**, 375-387.
9. **Ko LJ, Prives C.** p53: puzzle and paradigm. Genes Dev 1996 **10**, 1054-1072.
10. **Kohlenberg E, Payette JR, Sowa MG, Levasseur MA, Riley CB, Leonardi L.** Determining intestinal viability by near infrared spectroscopy: A veterinary application. Vib Spectrosc 2005, **38**, 223-228.
11. **Krishna CM, Kegelaer G, Adt I, Rubin S, Kartha VB, Manfait M, Sockalingum GD.** Combined Fourier transform infrared and Raman spectroscopic approach for identification of multidrug resistance phenotype in cancer cell lines. Biopolymers 2006, **82**, 462-470.
12. **Lim JK, Lee Y, Lee K, Gong M, Joo SW.** Reversible thermochromic change of molecular architecture for A diacetylene derivative 10,12-pentacosadiynoic acid thin films on Ag surfaces. Chem Lett 2007, **36**, 1226-1227.
13. **Liu C, Zhang Y, Yan X, Zhang X, Li C, Yang W, Shi D.** Infrared absorption of human breast tissues *in vitro*. J Luminescence 2006, **119-120**, 132-136.
14. **Maziak DE, Do MT, Shamji FM, Sundaresan SR, Perkins DG, Wong PTT.** Fourier-transform infrared spectroscopic study of characteristic molecular structure in cancer cells of esophagus: An exploratory study. Cancer Detect Prev 2007, **31**, 244-253.
15. **Meurens M, Wallon J, Tong J, Noël H, Haot J.** Breast cancer detection by Fourier transform infrared spectrometry. Vib Spectrosc 1996, **10**, 341-346.
16. **Mordechai S, Sahu RK, Hammody Z, Mark S, Kantarovich K, Guterman H, Podshyvalov A, Goldstein J, Argov S.** Possible common biomarkers from FTIR microspectroscopy of cervical cancer and melanoma. J Microsc 2004, **215**, 86-91.
17. **Romeo M, Diem M.** Correction of dispersive line shape artifact observed in diffuse reflection infrared spectroscopy and absorption/reflection (transflection) infrared micro-spectroscopy. Vib Spectrosc 2005, **38**, 129-132.
18. **Ruddon RW.** Cancer Biology. pp. 3-16, Oxford University Press, Oxford, 2007.
19. **Sindhuphak R, Issaravanich S, Udomprasertgul V, Srisookho P, Warakamin S, Sindhuphak S, Boonbundarlchai R, Dusitsin N.** A new approach for the detection of cervical cancer in Thai women. Gynecol Oncol 2003, **90**, 10-14.
20. **Sulé-Suso J, Skingsley D, Sockalingum GD, Kohler A, Kegelaer G, Manfait M, El Haj AJ.** FT-IR microspectroscopy as a tool to assess lung cancer cells response to chemotherapy. Vib Spectrosc 2005, **38**, 179-184.
21. **Torrance CJ, Agrawal V, Vogelstein B, Kinzler KW.** Use

of isogenic human cancers cells for high-throughput screening and drug discovery. Nat Biotechnol 2001, **19**, 940-945.
22. **Walsh MJ, German MJ, Singh M, Pollock HM, Hammiche A, Kyrgiou M, Stringfellow HF, Paraskevaidis E, Martin-Hirsch PL, Martin FL.** IR microspectroscopy: potential applications in cervical cancer screening. Cancer Lett 2007, **246**, 1-11.
23. **Wang HP, Wang HC, Huang YJ.** Microscopic FTIR studies of lung cancer cells in pleural fluid. Sci Total Environ 1997, **204**, 283-287.
24. **Wong PTT, Wong RK, Caputo TA, Godwin TA, Rigas B.** Infrared spectroscopy of exfoliated human cervical cells: evidence of extensive structural changes during carcinogenesis. Proc Natl Acad Sci USA 1991, **88**, 10988-10992.
25. **Zhang W, McClain C, Gau JP, Guo XYD, Deisseroth AB.** Hyperphosphorylation of p53 induced by okadaic acid attenuates its transcriptional activation function. Cancer Res 1994, **54**, 4448-4453.
26. **Zenobi MC, Luengo CV, Avena MJ, Rueda EH.** An ATR-FTIR study of different phosphonic acids in aqueous solution. Spectrochim Acta A Mol Biomol Spectrosc 2008, **70**, 270-276.